

SLAC-PUB-3335  
May 1984  
(T/E)

NEW PARTICLE SEARCHES AT PEP\*

H. R. Band  
Department of Physics  
Northeastern University, Boston, Massachusetts 02115  
and  
Stanford Linear Accelerator Center  
Stanford University, Stanford, California 94305

ABSTRACT

New particle searches by TPC, MARK II, and MAC are reviewed. No evidence of supersymmetric particle production has been seen in two possible reactions. Improved lower bounds on the  $\tilde{e}$  mass have been set. The TPC search for charge  $(4/3)e$  particles is reported.

Invited talk presented at the 1984 Rencontre de Moriond:  
Electroweak Interactions and Unified Theories, La Plagne, France,  
February 26 - March 4, 1984

---

\* Work supported by the National Science Foundation under contract NSF-PHY79-20821, and in part by the Department of Energy, contract DE-AC03-76SF00515.

## 1. Introduction

PEP has accumulated a large data base in recent years ( $> 200 \text{ pb}^{-1}$  per experiment) at a center of mass energy of 29 GeV. MAC and MARK II have exploited this large accumulated luminosity by searching for rare production modes of supersymmetric particles which probe  $\tilde{e}$  masses in excess of the beam energy. Such production modes may offer the cleanest evidence for supersymmetric particle production in the next few years if the  $\tilde{e}$  mass is less than  $50 \text{ GeV}/c^2$ .

The TPC group is searching for fractionally charged particles in multihadronic events. The first result of this search, limits on the production of charge  $(4/3)e$  particles, is presented.

## 2. Search for Charge $(4/3)e$ Particles

Most searches for particles of fractional charge have focussed on free quarks. However, some QCD models<sup>1)</sup> predict stable diquark states even if no free quarks are found. The TPC group has searched for charge  $(4/3)e$  diquarks ( $uu$ ) in hadronic final states.<sup>2)</sup>

The Time Projection Chamber (TPC) is a large cylindrical gas volume under high pressure with parallel electric and magnetic fields. Ionization from charged tracks drift to either end of the chamber where both the time and position of arrival are measured. A particle's charge is identified in the TPC by simultaneous measurement of the momentum and ionization. Up to 183 ionization measurements are collected per track. The  $\langle dE/dx \rangle$  assigned to each track is defined as the mean of the lowest 65% of the ionization pulse heights. For minimum ionizing pions a  $\langle dE/dx \rangle$  resolution of 3.9% and a momentum resolution of  $0.035p$  (GeV/c) were achieved.

Multihadronic events were identified by requiring five or more verticizing tracks with a total momentum greater than  $7.25 \text{ GeV}/c$  and a forward backward energy imbalance less than 40%. In a data sample of  $22 \text{ pb}^{-1}$ , 7137 hadronic events were found with an estimated background of 8%. The  $\langle dE/dx \rangle$  distribution of tracks from a subset of this sample is plotted in Fig. 1. Also shown are curves of expected  $\langle dE/dx \rangle$  as a function of momentum for stable particles.

A charge  $(4/3)e$  particle would have  $\langle dE/dx \rangle$  a factor of  $(4/3)^2$  larger than that of a charge  $1e$  particle and would populate the upper portion of Fig. 1. The search region for  $(4/3)e$  tracks was chosen to be outside the regions populated by known charge  $1e$  particles. Candidate tracks were required to be well measured ( $> 80$  ionization samples and an error in momentum  $< 10\%$ ). Of the 50 candidate tracks in the search region, 8 were rejected by requiring that the track point to the event vertex eliminating tracks coming from interactions in the beam pipe or pressure vessel wall. Unresolved pairs of high momentum tracks with only one track reconstructed or tracks with an energetic delta ray were a

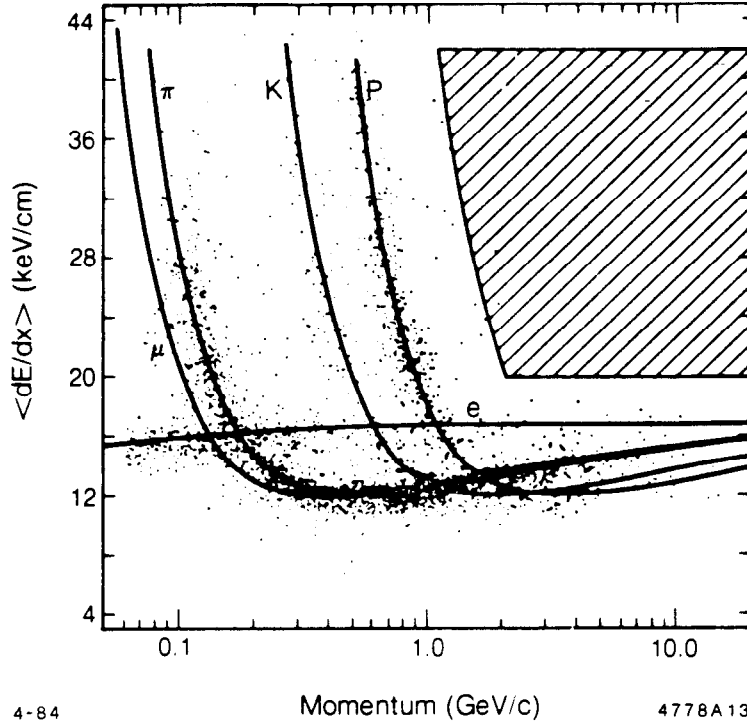


FIG. 1.  $\langle dE/dx \rangle$  vs. momentum for tracks from multihadronic events measured by the TPC. The expected  $\langle dE/dx \rangle$  vs. momentum correlations are shown as solid curves for several particle types. The search region for charge  $(4/3)e$  particles is shown as the cross-hatched area.

4-84

Momentum (GeV/c)

4778A13

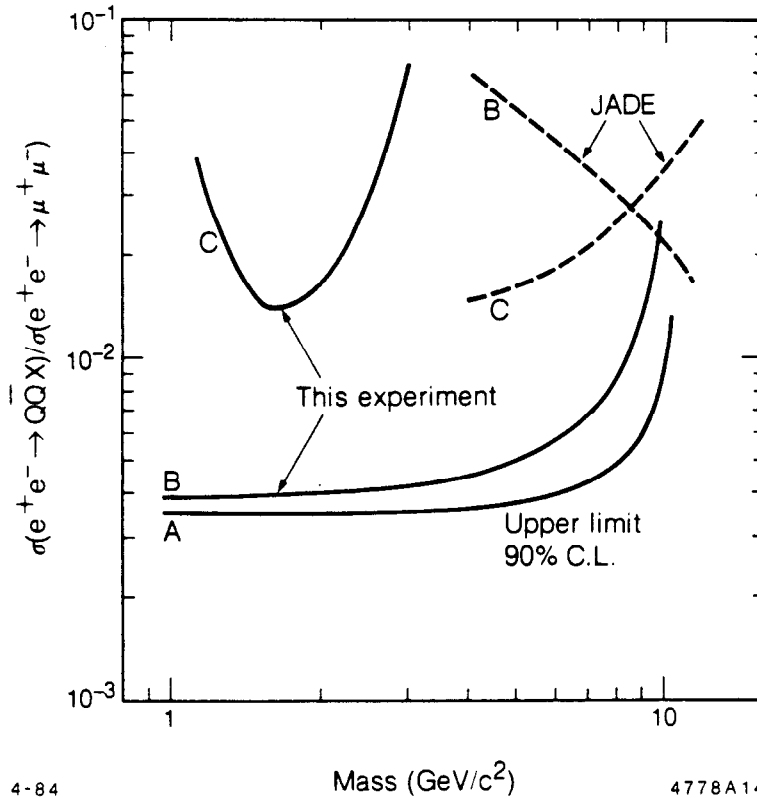


FIG. 2. Cross section limits from TPC for inclusive production of charge  $(4/3)e$  particles with the following momentum distributions:  
 (A)  $dN/dp \propto p^2/E$ ,  
 (B)  $dN/dp \propto \text{constant}$ , and  
 (C)  $dN/dp \propto (p^2/E) \cdot e^{-3.5E}$ .  
 The dashed curves are limits previously set by JADE.

4-84

Mass (GeV/c<sup>2</sup>)

4778A14

large background to the remaining tracks. In either case the ionization for part of the candidate track's length was doubled. To reject these tracks, cuts were made on the number of unassociated hits allowed near the track of interest. Additionally the track was required to have a statistically uniform ionization along its track length. No candidate tracks survived all of these cuts.

The detection efficiency of these cuts for charge  $(4/3)e$  tracks was determined from Monte Carlo studies to be  $72 \pm 10\%$ . The final cross section limit for  $(4/3)e$  particle ( $Q\bar{Q}$ ) production depends on the momentum ( $dN/dp$ ) distribution assumed. Limits for several momentum distributions are shown in Fig. 2. For a momentum spectrum similar to that of heavy hadrons the limit is  $R_Q < 0.005$  for  $1 < m_Q < 8 \text{ GeV}/c^2$ .

### 3. Supersymmetry Searches

#### A. Introduction

Much theoretical interest has been recently devoted to supersymmetric theories (SUSY) with several talks at this conference exploring different SUSY models. In SUSY there is a partner to every known particle which differs only in the spin (by  $1/2$ ). Thus the SUSY partner to the  $\gamma$  is the spin  $1/2$  photino  $\tilde{\gamma}$  and the partners to the electrons are the spin 0 selectrons  $\tilde{e}_R, \tilde{e}_L$  (one partner for each helicity state). It is known that SUSY cannot be an exact symmetry as no SUSY partners with mass equal to their standard model counterpart have been found. However, the masses of SUSY particles are not constrained by theory and SUSY particles may exist with masses within the range of PEP experiments.

Until this past year SUSY searches at  $e^+e^-$  machines have been limited to pair production processes in which the SUSY particle mass was less than the beam energy. The reported null results indicate  $m_{\tilde{e}}, m_{\tilde{\mu}} > 14.5 - 17 \text{ GeV}/c^2$ . The MAC and MARK II collaborations have searched for single  $\tilde{e}$  production in association with a  $\tilde{\gamma}$ . This reaction probes  $m_{\tilde{e}} < 2 E_{\text{beam}}$  if the  $\tilde{\gamma}$  mass is small. The MAC group has also searched for the reaction

$$e^+e^- \rightarrow \gamma\tilde{\gamma}\tilde{\gamma},$$

which is sensitive to  $\tilde{e}$  masses as high as  $50 \text{ GeV}/c^2$ .

#### B. Single $\tilde{e}$ Production, MARK II

The reaction studied is:

$$e^+e^- \rightarrow e^{\pm}\tilde{e}^{\mp}\tilde{\gamma}$$

followed by the decay  $\tilde{e}^{\mp} \rightarrow e^{\mp}\tilde{\gamma}$ . It is assumed that the  $\tilde{\gamma}$ 's are stable and only weakly interacting and are thus not seen in the detector. Calculations of this process<sup>3)</sup> show that the  $e^{\pm}$  in the final state is scattered by a very small angle and escapes undetected down the beam pipe. The only observed final state particle is the  $e^{\mp}$  from the  $\tilde{e}$  decay. This electron has high energy ( $\approx m_{\tilde{e}}/2$ ) and

an almost flat angular distribution.

The MARK II has searched for  $\tilde{e}$  production<sup>4)</sup> by examining events with single electrons and no other detected particles. The MARK II detector has been described elsewhere in detail.<sup>5)</sup> Electrons and photons are detected in the liquid argon (LA) calorimeter ( $|\cos\theta| < 0.7$ ), endcap calorimeters ( $0.75 < |\cos\theta| < 0.92$ ), and the endcap taggers ( $2^\circ < \theta < 4^\circ$ ). Both the LA and endcap calorimeters have azimuthal breaks in coverage due to structural supports. Charged particle detection is supplied by the central drift chamber (CD) and the vertex chamber to within  $10^\circ$  of the beam.

Single electron events were selected to have only one CD track with  $|\cos\theta| < 0.7$ . The track was also required to be  $> 2.7^\circ$  away from any azimuthal crack in the LA calorimeter. Events with any neutral energy unassociated with the CD track were also rejected. In a data sample of  $123 \text{ pb}^{-1}$ , 763 events were found with electron energy  $> 6 \text{ GeV}$ . Backgrounds from  $e^+e^-\gamma\gamma$  ( $0.9 \pm 0.5$ ),  $\tau^+\tau^-$  ( $< 0.6$ ), and two photon processes were small. The remaining background was  $e^+e^-\gamma$  events where one of the electrons is undetected at very small angles and the  $\gamma$  hits an uninstrumented crack between calorimeter elements. The procedure used to eliminate these events was to fit the event to the  $e^+e^-\gamma$  hypothesis assuming the unseen electron is at  $\theta = 0^\circ$ . If the fitted angles of the gamma pointed to an area of the calorimetry where the detection efficiency was not 100%, the event was rejected. Checks of the reliability of this method were made by fitting events where both the  $e$  and  $\gamma$  were observed. A comparison of the difference between the fitted and measured values is shown in Fig. 3, where the difference has been divided by the error in the predicted angles.

All 763 candidate events were fitted to the  $e^+e^-\gamma$  hypothesis. The predicted  $\gamma$  angles are shown in Fig. 4. Any event with a predicted  $\gamma$  angle with

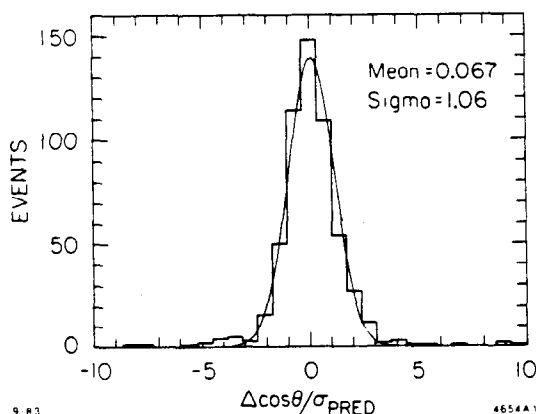


FIG. 3. The normalized error distribution in the predicted  $\gamma \cos\theta$  for events with one observed electron and photon. The  $\gamma$  angles were predicted from fits to the  $ee\gamma$  hypothesis.

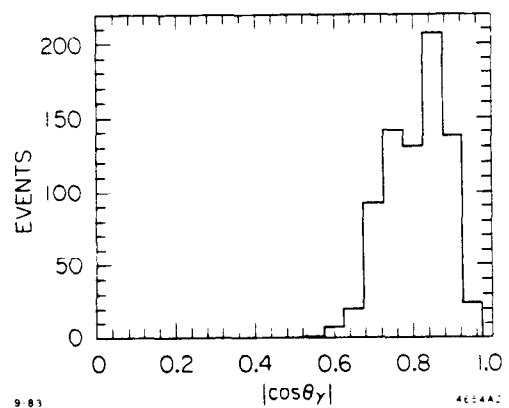


FIG. 4. Distribution of the predicted  $\gamma |\cos\theta|$  for single electron candidates in MARK II.

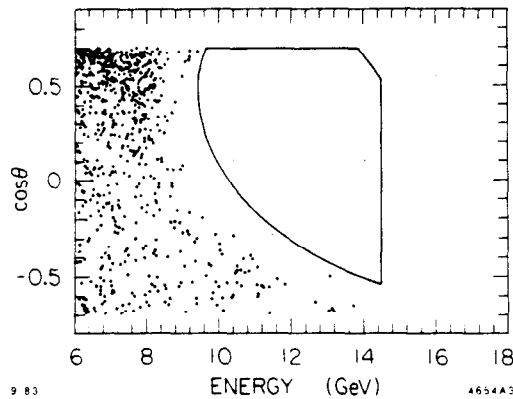


FIG. 5. The search region for single electrons from  $\tilde{e}$  decay in MARK II. For positive tracks  $\cos\theta$  has been plotted as  $-\cos\theta$ .

$|\cos\theta| > 0.54$  was rejected. The effect of this cut was to define a search region in the energy vs.  $\cos\theta$  plane as shown in Fig. 5. No single electrons were found in this search region. The efficiency for detecting an electron from a  $\tilde{e}$  decay was calculated to be 41% in the search region. This places an upper limit on the cross section in the search region of  $2.7 \cdot 10^{-2}$  pb. If the masses of  $\tilde{e}_L$  and  $\tilde{e}_R$  are equal, the corresponding lower limit on the  $\tilde{e}$  mass is  $22.2 \text{ GeV}/c^2$  at the 95% confidence level. (When the masses of the SUSY

partners are not equal, for example  $m_{\tilde{e}_R} \gg m_{\tilde{e}_L}$ , then only the lightest partner contributes to the cross section and the mass limit becomes  $m_{\tilde{e}_L} > 19.4 \text{ GeV}/c^2$ .)

### C. Single $\tilde{e}$ Production, MAC

The MAC detector<sup>6)</sup> is well suited for the study of reactions with missing energy and momentum. The detector consists of a cylindrical drift chamber (CD) surrounded by a hexagonal barrel of electromagnetic calorimeters, scintillation counters, and hadronic calorimeters. Planar endcap scintillators and calorimeters extend the coverage to small angles from the beam. Several layers of drift tubes outside the central and endcap calorimeters provide muon identification and tracking. MAC is essentially 100% efficient at detecting energetic photons and electrons ( $> 2 \text{ GeV}$ ) to within  $9^\circ - 12^\circ$  of the beam. Its detection coverage was extended by the installation of veto calorimeters covering  $5^\circ < \theta < 17^\circ$  during the summer of 1983. Unobserved particles in the  $e^+e^-\gamma$  final state are confined to small angles about the beam. The energy and angular distributions of the observed  $e(\gamma)$  are thus severely restricted by momentum conservation.

The single electron analysis covered two data samples. In the first data sample of  $36.4 \text{ pb}^{-1}$ , showering particles could be detected to within  $9^\circ - 12^\circ$  of the beam. In the second data sample of  $29.5 \text{ pb}^{-1}$ , taken after the installation of the veto calorimeters, showering particles could be detected to within  $5^\circ$  of the beam. The analysis required a CD track with  $|\cos\theta| < 0.75$ , momentum  $> 1.0 \text{ GeV}/c$ , and associated electromagnetic shower energy  $> 3 \text{ GeV}$  ( $2 \text{ GeV}$  for the second data sample). Events with more than one CD track or shower were rejected, leaving 1565 events from the first data sample.<sup>7)</sup> The energy (Fig. 6) and angular distributions of these events are consistent with the expected distributions from  $e^+e^-\gamma$  events. The overall trigger and analysis efficiency for the single electron events was calculated as 92% at  $3 \text{ GeV}$  and 95%

at or above 6 GeV. Electrons produced by the  $\tilde{e}$  decay were expected to have energies  $> 7$  GeV (see Fig. 6) and not to overlap the region populated by the  $e\bar{e}\gamma$  background.

The energies measured in the veto calorimeters for single electron events in the second data sample are shown in Fig. 7. Events with veto calorimeter energy  $> 0.25$  GeV were rejected as  $e\bar{e}\gamma$  background. Studies of veto calorimeter noise indicate that  $< 1.4\%$  of the true  $\tilde{e}$  events would fail this cut. The electron energy distribution of the two data samples are compared in Fig. 8. The veto energy cut clearly suppressed the  $e\bar{e}\gamma$  background reducing the maximum observed electron energy to 3 GeV. Utilizing the combined data sample, the upper limit on the single electron cross section in the MAC search region was  $< 0.048$  pb at the 95% confidence level. As can be seen from Fig. 9, which shows the  $\tilde{e}$  cross section in the MAC acceptance as a function of mass, the corresponding mass limit is  $m_{\tilde{e}} > 23.4$  GeV/c<sup>2</sup> (22.1 GeV/c<sup>2</sup>). Future increases in the MAC data sample will only marginally improve the  $\tilde{e}$  mass limit. Further improvements on the  $\tilde{e}$  mass limit will necessarily be made at higher beam energies or with different reactions. The JADE group has reported at this conference a preliminary limit of 25 GeV/c<sup>2</sup> based on the single electron technique.<sup>8)</sup>

#### D. $\tilde{\gamma}\tilde{\gamma}$ , MAC

The second SUSY reaction studied was

$$e^+e^- \rightarrow \gamma\tilde{\gamma}$$

which has been suggested by various authors.<sup>9,10)</sup> The cross section for this reaction, which proceeds by virtual  $\tilde{e}$  exchange, is a function of both the  $\tilde{e}$  and  $\tilde{\gamma}$  mass. Recently several authors have published calculations of the cross section<sup>11,12,13)</sup> for arbitrary  $\tilde{e}$  and  $\tilde{\gamma}$  masses. As in the single electron search, the  $\tilde{\gamma}$ 's are assumed stable, thus the only observed particle is a  $\gamma$  with missing energy and momentum. A reaction experimentally indistinguishable from the  $\tilde{\gamma}\tilde{\gamma}$  process is

$$e^+e^- \rightarrow \nu\bar{\nu}\gamma$$

in which the neutrinos are, of course, unobserved. The cross section<sup>14)</sup> for this process has also been calculated with the only uncertainty being the number of light neutrino flavors. Measurements of the single photon spectrum will either measure or place limits on  $N_\nu$  as well as  $m_{\tilde{\gamma}}$ .  $N_\nu = 3$  was assumed for estimating the  $\nu\bar{\nu}\gamma$  contribution in the  $\tilde{\gamma}\tilde{\gamma}$  search. The cross sections for these processes are shown in Fig. 10 for  $m_{\tilde{\gamma}} = 1$  GeV/c<sup>2</sup>,  $N_\nu = 3$ , and several  $\tilde{e}$  masses as a function of  $\sqrt{s}$ . Although the cross section for  $\tilde{\gamma}\tilde{\gamma}$  rises with energy, it is clear that for large  $\tilde{e}$  masses the signal to background ratio is better at lower energies. Thus this reaction seems ideally suited for study at PEP.

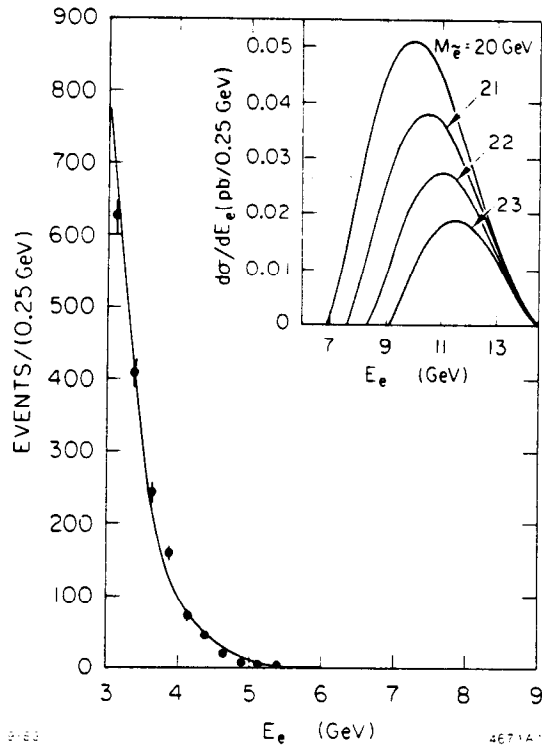


FIG. 6. Energy distribution of single electron events found by MAC in a data sample of  $36.4 \text{ pb}^{-1}$ . The predicted background from  $ee\gamma$  final states is shown as the solid curve. The expected energy distribution of electrons from  $\tilde{e}$  decay is shown in the inset.

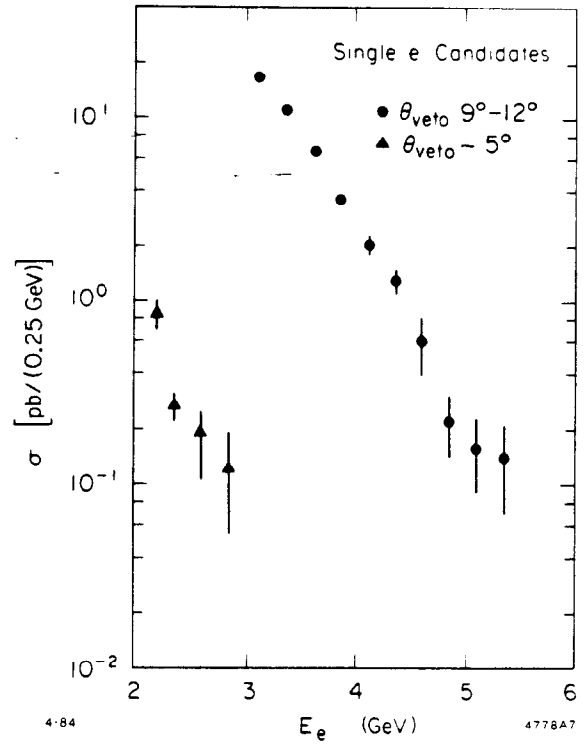


FIG. 8. Energy distributions of single electron events. In first data sample of  $36.4 \text{ pb}^{-1}$  (solid dots), electrons and photons from  $e^+e^-\gamma$  could be detected to within  $9^\circ$ - $12^\circ$  of the beam. In the second data sample of  $29.5 \text{ pb}^{-1}$  (solid triangles), electrons and photons could be detected to within  $5^\circ$  of the beam.

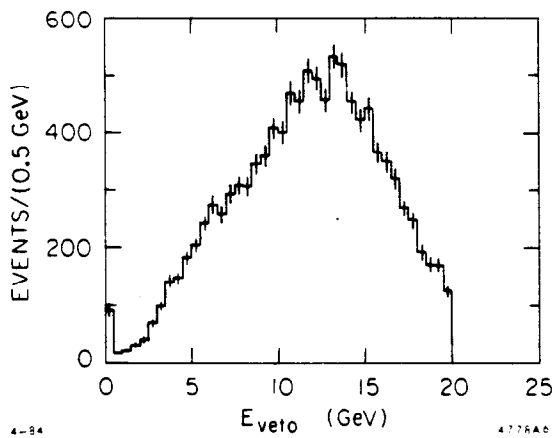


FIG. 7. Energy distribution in the veto calorimeters covering  $5^\circ$ - $17^\circ$  for single electron candidates in a data sample of  $29.5 \text{ pb}^{-1}$ . Events with  $E_{\text{veto}} > 0.25 \text{ GeV}$  were rejected as  $ee\gamma$  background.

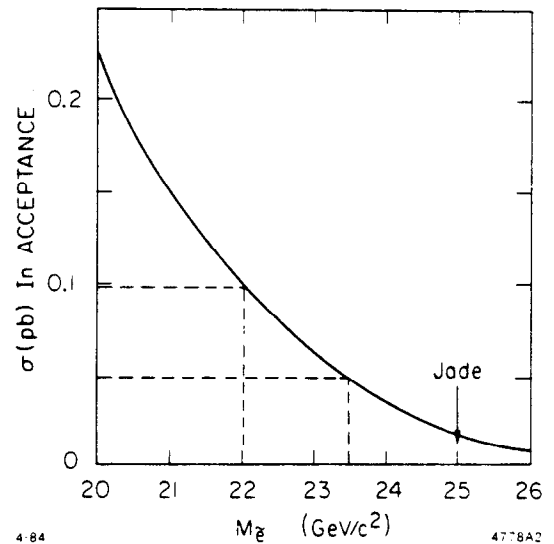


FIG. 9. Cross section in the MAC acceptance of electrons from  $\tilde{e}$  decays as a function of the  $\tilde{e}$  mass. The MAC upper limit of  $0.048 \text{ pb}$  corresponds to  $m_{\tilde{e}} > 23.4 \text{ GeV}/c^2$ .



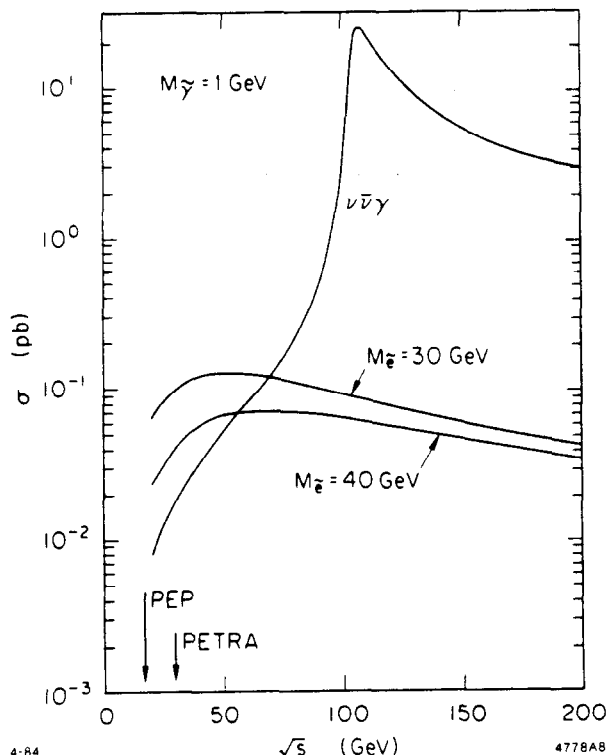


FIG. 10. Cross sections for single  $\gamma$  events from the reactions  $e^+e^- \rightarrow \tilde{\nu}\tilde{\nu}\gamma$ , and  $e^+e^- \rightarrow \nu\bar{\nu}\gamma$  assuming  $N_\nu=3$ ,  $m_\gamma=1 \text{ GeV}/c^2$ ,  $E_\gamma > 0.2 E_{\text{beam}}$ , and  $|\cos\theta| < 0.94$ .<sup>11)</sup>

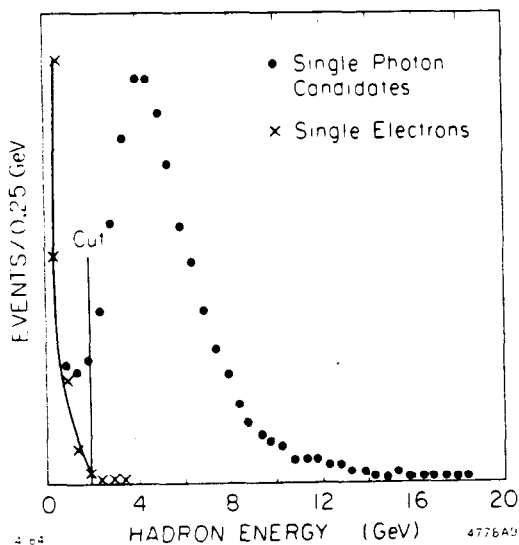


FIG. 11. Hadronic energy of single electron and photon candidates. A cut of  $< 2 \text{ GeV}$  eliminates most of the cosmic ray background to the single photons.

Other backgrounds to the single photon final state are in principal distinguishable from the signal. There are, in analogy to the single electron events, single photons from  $ee\gamma$  events in which the  $\gamma$  is observed and the electrons ( $e^\pm$ ) are unobserved at small angles. As in the single electron analysis, the energy and angular distributions of the  $\gamma$ 's for  $ee\gamma$  are constrained and single photon search regions can be defined so that this background is negligible. Other potentially troublesome backgrounds are cosmic ray events and proportional chamber noise which sometimes look similar to photon showers.

The data analysis cuts required a photon shower with  $40^\circ < \theta < 140^\circ$  and  $\phi > 3^\circ$  from a sextant boundary. No CD tracks were allowed. Events with more than one shower in excess of one GeV were rejected. The hadronic energy of the events passing these cuts is shown in Fig. 11. A cut of  $< 2 \text{ GeV}$  of hadronic energy eliminated most of the cosmic ray events while rejecting 2% of the real  $\gamma$ 's. Further cuts required the photon shower point back to the interaction point and have a width and longitudinal development compatible with known electron showers. Two data samples of differing small angle detection efficiency were again studied. As in the electron analysis, a veto calorimeter energy cut of  $0.25 \text{ GeV}$  was used in the second data sample.

The observed  $p_\perp$  distributions of the two data samples are compared in

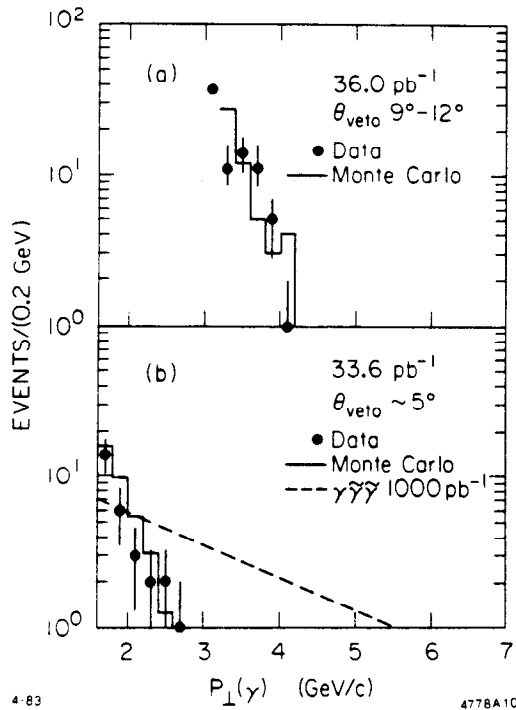


FIG. 12.  $p_{\perp}$  distributions of single photon candidates selected as described in the text. The expected background from  $ee\gamma$  events is shown as solid curves. The background level is a function of the minimum polar angle at which tracks can be detected hence vetoing the single  $\gamma$  candidate. In (a) the veto angle was  $9^{\circ}$ - $12^{\circ}$ . The data in (b) had a veto angle of  $\sim 5^{\circ}$ . For reference the distribution of  $\gamma$ 's from  $\tilde{\gamma}\tilde{\gamma}$  events is also shown.

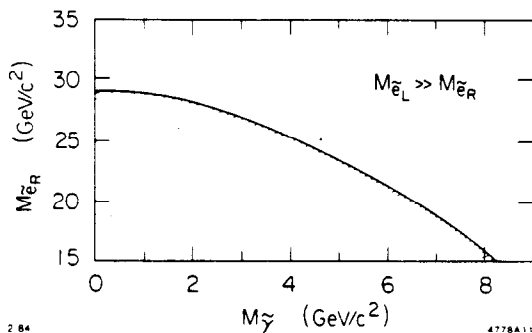


FIG. 13. The region in the  $m_{\tilde{e}}$  vs.  $m_{\tilde{\gamma}}$  plane excluded by the MAC measurements assuming one of the  $\tilde{e}$  partners is very massive. If the  $\tilde{e}$  masses are identical, the excluded region is larger.

Figs. 12a and 12b with the expected  $ee\gamma$  background. The search region was defined as  $p_{\perp} > 4.3$  GeV/c for the first sample and as  $p_{\perp} > 3.0$  GeV/c for the second. As seen in Fig. 12, a significant fraction of the photons from  $\tilde{\gamma}\tilde{\gamma}$  can have  $p_{\perp}$  inside the search regions. The overall trigger and analysis efficiency for detecting these  $\gamma$ 's in either search region was 70%. No candidate photons were found in the search region. This sets an upper limit on  $N_{\tilde{\gamma}} < 43$ . If the  $\tilde{\gamma}$  mass is zero, the lower limit on the  $\tilde{e}$  mass is  $> 35$  GeV/c<sup>2</sup> ( $> 29$  GeV/c<sup>2</sup>) at the 90% confidence level. The excluded masses for the more general case of nonzero  $\tilde{\gamma}$  mass can be seen in Fig. 13. MAC expects to double its sensitivity to the  $\tilde{\gamma}\tilde{\gamma}$  cross section by this summer. If no candidates are found, the lower limit on the  $\tilde{e}$  mass would increase to 40-50 GeV/c<sup>2</sup>.

#### 4. Conclusion

No evidence of fractional charge or supersymmetric particle production has been observed by PEP detectors. The  $\tilde{e}$  mass has been constrained to be  $> 35$  GeV/c<sup>2</sup> at the 90% confidence level. Negative searches for associated  $\tilde{e}\tilde{\gamma}$  production give similar though smaller mass limits. Continued studies of the  $\tilde{\gamma}\tilde{\gamma}$  final may probe  $\tilde{e}$  masses in the 40-50 GeV/c<sup>2</sup> range in the coming year.

## ACKNOWLEDGMENT

I would like to thank the TPC, MARK II, and MAC collaborations for supplying their latest results.

## REFERENCES

- 1) R. Slansky, T. Goldman and G. Shaw, Phys. Rev. Lett. 47, 887 (1981).
- 2) H. Aihara, et al., Phys. Rev. Lett. 52, 168 (1984).
- 3) M. K. Gaillard, L. Hall, and I. Hinchliffe, Phys. Lett. 116B, 279 (1982).
- 4) L. Gladney, et al., Phys. Rev. Lett. 51, 2253 (1983).
- 5) R. H. Schindler, et al., Phys. Rev. D 51, 78 (1981).
- 6) W. T. Ford in Proceedings of the International Conference on Instrumentation for Colliding Beams, edited by W. Ash, Report No. SLAC-250, 1982.
- 7) E. Fernandez, et al., Phys. Rev. Lett. 52, 22 (1984).
- 8) G. Flügge, "Search for New Particles at Petra," Proceedings of the XIXth Rencontre De Moriond Conference on Electroweak Interactions and Unified Theories, La Plagne, France, February 26-March 4, 1984.
- 9) P. Fayet, Phys. Lett. 117B, 460 (1982).
- 10) J. Ellis and J. S. Hagelin, Phys. Lett. 122B, 303 (1983).
- 11) K. Grassie and P. N. Pandita, DO-TH 83/25.
- 12) J. Ware and M. E. Machacek, NUB 2626 (1984).
- 13) T. Kobayashi and M. Kurada, TPR-83-22 (1984).
- 14) E. Ma and J. Okada, Phys. Rev. Lett. 41, 287 (1978), and K. J. F. Gaemers, R. Gastman, and F. M. Renard, Phys. Rev. D 19, 1605 (1979).